Equilibrium models for two samples of OH/IR stars

Te Lintel Hekkert, P.; Dejonghe, H.; Habing, H.J.

Equilibrium Models for two Samples of OH/IR Stars

P. te Lintel Hekkert, *Mount Stromlo and Siding Spring Observatories, Private Bag, Weston ACT 2611*
H. Dejonghe, *Sterrenkundig Observatorium, Rijks Universiteit Gent, Krijgslaan, Gent, Belgium*
H. J. Habing, *Sterrewacht Leiden, Leiden, The Netherlands*

Abstract: We present a progress report on the dynamical analysis of the *IRAS* sample of OH/IR stars. This sample is complete within a distance of 8 kpc. We distinguish two groups of OH/IR stars, one with high and the other with low expansion velocity of the circumstellar shell.

Using a quadratic programming method we fit a database of Galactic orbits to the observed distribution of radial velocities, longitudes and latitudes. The dynamical model yields a distribution function, based on two integrals of motion, for each group. Integration gives the density, the mean velocity and the velocity dispersions as function of R and z. The distribution functions for the two groups differ enough to suggest that they represent two different stellar populations.

We estimate the stellar lifetime for each group by comparing the velocity dispersions and z scale-heights at the solar radius with those found for local stellar populations. We conclude that the group with the low expansion velocity is likely to be part of the thick disc, while the high expansion velocity group has dynamical characteristics resembling an old disc population; this in contrast with the findings for differently selected samples of OH/IR stars (e.g., Baud *et al.* 1981a; 1981b), which were found to be less than 1 Gyr old.

1. Introduction

In this paper, we give a progress report on a dynamical analysis of a new sample of OH/IR stars. The sample is based on the *IRAS* point source catalogue. OH/IR stars are excellent candidates to probe the dynamical structure of the bulge and halo. We perform a dynamical analysis of the data using a quadratic programming technique (QP; Dejonghe 1989, hereafter paper I). This method enables us to consider quite general distribution functions with as little prejudice as practical on their functional form.

OH/IR stars are highly evolved objects located on the tip of the Asymptotic Giant Branch (AGB). They are very luminous (typically $L_* \approx 4500\ L_\odot$). The progenitors are thought to have Zero Age Main Sequence (ZAMS) masses between 1 and 3 $M_\odot$, and OH/IR stars therefore are older than 1.5 Gyr. The OH/IR stars lose mass at a very high rate ($> 10^{-6}\ M_\odot\ \mathrm{yr}^{-1}$). The associated dust and gas forms a nearly spherical, high opacity shell around the star. Nearly all the energy from the star is converted by the dust shell into infrared radiation at wavelengths between 5 and 60 μm. The conditions in the dust shell are favourable for the OH 1612 MHz maser, which is sufficiently powerful that stars can be detected that are beyond the Galactic centre. During an all-sky survey the *IRAS* satellite found essentially all AGB stars in the infrared, although within 2° from the Galactic plane only a very small percentage could be identified due to confusion. Detection of the 1612 MHz line in the directions of the newly found AGB stars gives us their radial velocities.

The 1612 MHz line profiles typically show two sharp peaks. The mean radial velocity of the spikes is the stellar velocity; the velocity difference (ΔV) is twice the expansion velocity of the dust shell (e.g., Olnon 1977). Samples differentiated on the basis of the expansion velocity show differences in kinematic and Galactic distribution (Baud *et al.* 1981a, 1981b; Olnon *et al.* 1981). Thus it is possible to use the expansion velocity as an indicator for the ZAMS mass (and lifetime) of the star, at least in a statistical sense. Baud *et al.* (1981b) concluded that OH/IR stars with larger expansion velocities are part of a younger population than the OH/IR stars with smaller expansion velocities. Since we are dealing with an old disc-thick disc (as we will show in this paper) population a model composed solely of circular orbits is not adequate. In order to recover the physical parameters describing the population from the observed projected information, we make use of the general theory of equilibrium models of stellar systems.

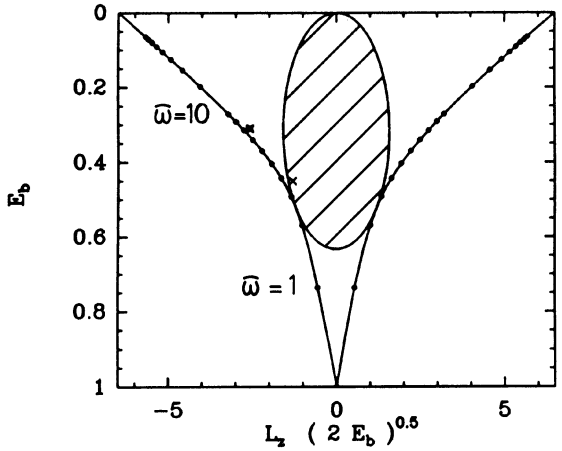

Figure 1 – Phase space, based on two integrals of motion: E_b and L_z. The E_b co-ordinate is scaled between zero and one and the $L_z\sqrt{2E_b}$ coordinate is scaled accordingly. The loci of circular orbits, which define the outer boundary of phase space, are indicated. (Every $E_b \neq 0$ gives $\pm L_{z,max}$ corresponding with circular orbits.) The boundary of space phase is characterised by the potential. On the boundary the circular orbits (per definition at $z = 0$) at each 1 kpc till 10 kpc and further each 5 kpc till 50 kpc from the centre are indicated with • (the circular orbits at 1 kpc and 10 kpc are indicated). For a given position (ϖ, z), the region that is accessible in phase space is bounded by an ellipse. The case for (ϖ, z) = (2.5 kpc, 0.0 kpc) is indicated (shaded area). An example of an orbit is given in Figure 2 corresponding with (E_b, L_z) = (0.45, −1.30) (indicated with a cross).

A dynamical model consists of a potential and a distribution function of the orbital parameters. By generating best fitting models, we can obtain information on the parameters of the potential, such as scale lengths. In this paper we will assume an axisymmetric potential, ψ, for the Galaxy (Dejonghe and de Zeeuw 1988) and then determine the most pronounced features of the distribution function for the samples of OH/IR stars. Since the sample covers a large volume in space (almost half of the Galaxy), it is unlikely that extrapolation of our models in phase space will be very critical, in contrast to models derived from star counts in the solar neighbourhood.

A stellar system is adequately described by its distribution function F and its potential $\psi(\varpi, z)$. Our models are not self consistent, since we do not assume that the OH/IR stars form a selfgravitating stellar system; therefore the potential bears no direct relation to the population we are interested in, and F and ψ are quite independent.

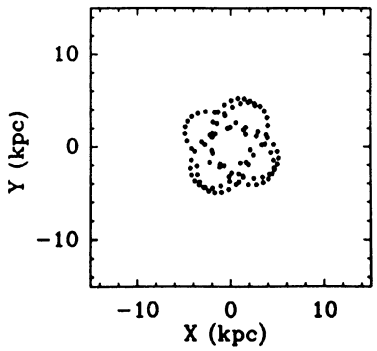

Figure 2 – An orbit in the Galactic plane with $E_b = 0.45$, $L_z = -1.30$. The energy and angular momentum were chosen to be close to the boundary of phase space (see Figure 1: cross).

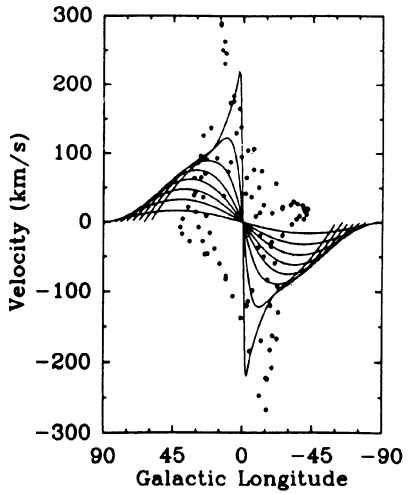

Figure 3 – The longitude–velocity diagram for the orbit in Figure 2. The lines in the longitude–velocity diagram are the projected velocities and longitudes for stars on circular orbits at given radius from the Galactic centre (at 1, 2, 3, ...7 kpc), assuming the rotation curve by Burton and Gordon (1978).

Our goal obviously will be to obtain information on the dynamics of our Galaxy in general, and more particularly on the dynamics of the population defined by our sample. The models may eventually enable us to constrain models of the formation history and future of the Galaxy. They will also yield suitable initial conditions for N-body experiments, which could be used to study the stability of the system.

Throughout the paper, we assume a solar distance from the Galactic Centre of 8 kpc (Feast 1987).

2. The Use of L_z and E_b in a Distribution Function

The stellar orbits, which will be used in section 4 to build the database, will be described in terms of integrals of motion. This is possible if we assume – as we will do – that the population of OH/IR stars are dynamically relaxed and in equilibrium in the Galactic potential. In an axisymmetric potential one can find generally three integrals of motion: the binding energy (E_b), angular momentum (L_z) along the symmetry (= rotation) axis, and the so called third integral (I_3), for which in general there is no simple expression.

The distribution of stars over space and velocities can be described (assuming an axisymmetric stellar system in equilibrium) by the function: $F(\mathbf{x}, \mathbf{v}, t) = F(\mathbf{x}, \mathbf{v})$ and by Jeans' theorem (e.g., Binney and Tremaine 1987): $F(\mathbf{x}, \mathbf{v}) = F(E_b, L_z, I_3) \approx F(E_b, L_z)$ with, in cylindric co-ordinates $E_b = \psi - (v_\varpi^2 + v_\phi^2 + v_z^2)/2$ and $L_z = \varpi v_\phi$. In the last step in this sequence of identities we state that F is independent of I_3 (i.e., we assume that all possible values of I_3 are equally probable). In general, the distribution function could be a function of three isolating integrals of the motion. Our dataset, however, is largely confined to the disc ($|b| < 10°$) and consists of projected densities and radial velocities only. Therefore we are almost completely ignorant about the velocity component in the z-direction for the stars in our sample. Thus we lack an important discriminating factor to constrain three-integral dynamical models. Therefore we expect that it must be possible to construct dynamical models that are compatible with the data and are only two-integral models. An important implication is that the velocity dispersions in the radial direction are equal to those in the z–direction at any given point in the Galaxy.

Figure 1 shows phase space. The co-ordinate E_b is intrinsically finite, but L_z is not. However, we make phase space finite by representing it in the co-ordinates E_b and $L_z\sqrt{2E_b}$. For a given position (ϖ, z), the region that is accessible in phase space is bounded by an ellipse. One case is indicated. It is clear that the local kinematics are influenced by the global potential, thus it is necessary to consider F entirely. In the extreme case, the (almost) circular orbit model, only the two boundaries of phase space are populated (the co- and counter-rotators with respect to the solar motion). Since the Galactic rotation occurs with negative L_z, we expect that most orbits will be close, but just to the right of the left locus of circular orbits.

In Figure 2 an orbit is sketched in the Galactic plane with given E_b and L_z. The projected velocities for this orbit is given in Figure 3. It is clear that a star with E_b and L_z just away from the boundary will have an orbit strongly deviating from circular; the distribution function thus is very sensitive to non-circular orbits.

3. The OH/IR Stars Database

The database consists of about 1500 OH/IR stars. For each star we know three parameters: Galactic longitude and latitude and the velocity projected along the line of sight. There is no distance information available for individual stars. Thus the six phase space co-ordinates ($\mathbf{x}$ and $\mathbf{v}$) are reduced to three, projected, quantities. It is obvious that the problem of finding the phase space distribution from this database is underdetermined. The (nearly complete) lack of sources $|b| < 2°$ makes the problem of finding the distribution function even harder. Nevertheless, the OH/IR stars are the best candidates to play this game, since they are luminous *and* the surveys of OH/IR stars are less biased than any other stellar survey. Although only projected stellar velocities are known, it is clear from the longitude–velocity diagrams (Figure 5) that simple kinematical models of circular orbits do not suffice in explaining the observed velocity distribution, but that orbits such as those in Figure 2 are required. However, the technique of quadratic programming allows us to select effectively orbits from a general database.

We used the following catalogues of 1612 MHz maser emission surveys of *IRAS* point sources (PSC): Eder *et al.* (1988), te Lintel Hekkert *et al.* (1989a, 1989b) and Sivagnanam and Le Squeren (1986). These catalogues are based on the PSC from

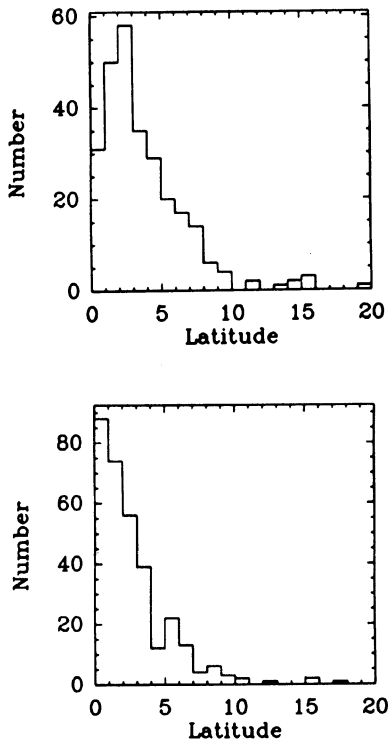

Figure 4: *Top* – The latitude distribution for the group I OH/IR stars. *Bottom* – As above, for the group II OH/IR stars.

which positions were selected on basis of infrared colours, fluxes and *IRAS* flux qualities (see *IRAS* Explanatory Supplement (hereafter ES), V.H.5). All of these catalogues are flux-limited samples, the survey by te Lintel Hekkert *et al.* 1989a reaching about 3 Jy at 12 μm; the others go deeper. The surveys overlap each other in the following area ($R21 = \log(f_{25\mu m}/f_{12\mu m})$) : $0.0 < R21 < 0.9$ and $f_{12\mu m} > 3.0$ Jy; thus we selected from the three catalogues the stars within these ranges. The bolometric correction, BC ($f_{tot} = BC \times \nu f_{12\mu m}$), does not vary more than 20% in the range of $R21$ (0.0 to 0.9). Further, we selected all OH/IR stars with $f_{12\mu m} > 3$ Jy and that are outside the Galactic areas where *IRAS* was confusion limited.

We divided the database into two equally sized groups; group I with $\Delta V < 27.25\,\mathrm{km\,s^{-1}}$ and group II having $\Delta V > 27.25\,\mathrm{km\,s^{-1}}$. In Figures 4 and 5 we show the latitude distribution and the longitude–velocity diagrams respectively. The latitude distribution is significantly different for the two samples, group II stars being much more confined to lower latitudes. In the longitude–velocity diagrams the group I sources are much more scattered than the group II sources: in group I about the same number of sources have velocities inside as outside the permitted zone. Nearly all the group II sources have radial velocities, allowed by circular differential rotation. From the longitude–velocity diagram we estimate that the velocity dispersions for group I and group II are at least 30 and $15\,\mathrm{km\,s^{-1}}$ respectively. We will assume that the *IRAS* database selected for the 1612 MHz surveys belongs to a population which can be described by a single luminosity function. Since the luminosity function for OH/IR stars is unknown, we have to assume one. For our models we only need to know the integrated luminosity function. We will assume a luminosity of 4700 $L_\odot$ for all OH/IR stars in our database; 4700 $L_\odot$ is the maximum of the luminosity function for the AGB stars in the Bulge (Habing 1987). The differences in luminosity between group I and II are unknown, but they are smaller than 35% and thus do not influence our modelling. A 4700 $L_\odot$ star will have a $f_{12\mu m} = 3$ Jy at 8 kpc, assuming a mean $BC = 3.4$ (van der Veen and Breukers 1989; Herman 1988). On the basis of these numbers we conclude that we sample half of the Galactic volume.

4. Building and Finding the Distribution Function

Moving along their orbits, stars will spend different amounts of time in different places according to their orbital velocity. Integrating along the line of sight, counting the number of stellar orbits crossing the line of sight (weighted with the occupation time) will give the projected densities and (radial) velocities. These model projections can be compared with the observations, and by tuning the number and kinds of orbits in the model Galaxy one will obtain a best-fitting model. Obviously, the weighted sum of all the orbital parameters of the model stellar orbits equals the distribution function: $F(\mathbf{x},\mathbf{v}) = F(E_b, L_z)$.

We use a potential with a rotation-curve that is essentially flat from 4–15 kpc, with circular velocity $v_c = 220\,\mathrm{km\,s^{-1}}$ (Dejonghe and de Zeeuw 1988). The rotation-curve of their potential is a fit to the rotation of the Bahcall–Schmidt–Soneira (1982) model. The latter is based on the observed rotation-curve of H I and CO gas line emission from the inner Galaxy.

The distribution function has the form

$$F(E_b, L_z) = \sum c_i F_i(E_b, L_z),$$

with $i = i(\alpha, \beta, \gamma)$. We will call $F_i(E_b, L_z)$ the 'building blocks' of the distribution function. We used two building-block 'families', based on simple Fricke–type polynomials (1952), which in our case take the form:

$$F^1_{\alpha,\beta,\gamma}(E_b, L_z) = {E_b}^\alpha\,(E_b {L_z}^2/2)^\beta\,(AL_z\sqrt{2E_b} + BE_b + C{E_b}^2)^\gamma$$

$$F^2_{\alpha,\beta,\gamma}(E_b, L_z) = {E_b}^\alpha\,(E_b {L_z}^2/2)^\beta \left(\frac{E_b}{{E_b}^*\{L_z\}}\right)^\gamma$$

with ${E_b}^*\{L_z\}$ equal to the binding energy of the circular orbit for given L_z. Within each family A, B and C have fixed values; we only vary α, β and γ during the fitting procedure. A, B and C are so chosen, that each building block represents a distribution parallel to the loci of circular orbits. Each building block is used twice, representing stars that are rotating clockwise (negative L_z, hereafter co-rotating (with respect to the solar motion)) and counter-clockwise (positive L_z, hereafter counter-rotating (with respect to the solar motion)). Each family represents a different type of orbit. The first family is suitable to produce models which are slow rotating and have high velocity dispersion (typical velocity dispersion for this: 30–70 $\mathrm{km\,s^{-1}}$). These models have larger scale-heights than the models produced with the second family: typically 1500 pc. For models produced with second family building blocks typical velocity dispersions are: 10–20 $\mathrm{km\,s^{-1}}$. The scale-height of these models is smaller than for the family one models: 100–300 pc. The distribution functions built with these two families produce models with a wide range of kinematical characteristics.

Consider an observed quantity $\mu_{ob}(\mathbf{x}, \mathbf{v})$ that can be estimated by the mean of a function $\mu(\mathbf{x}, \mathbf{v})$ over some volume in phase space τ_l:

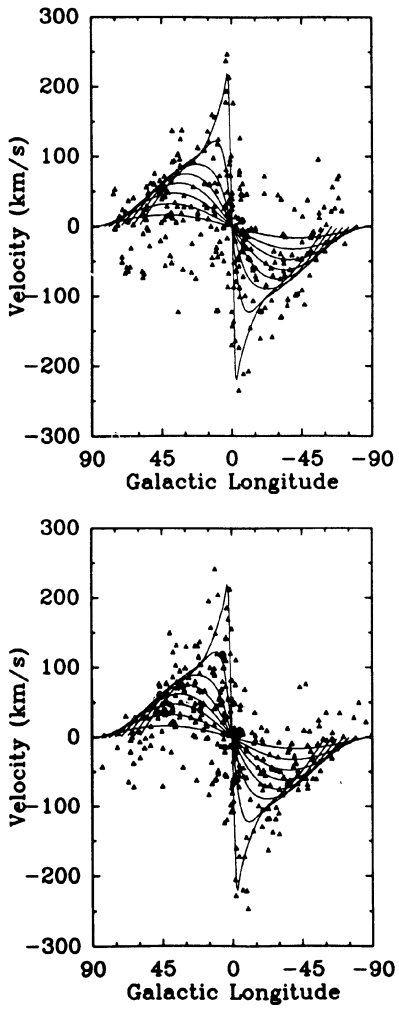

Figure 5: *Top* – The longitude–velocity diagram for the group I OH/IR stars. *Bottom* – As above, for the group II OH/IR stars. The lines in the longitude–velocity diagram are the projected velocities and longitudes for stars on circular orbits at given radius from the Galactic centre (at 1, 2, 3, ... 7 kpc), assuming the rotation curve by Burton and Gordon (1978). Since nearly all OH/IR stars are within the solar circle it is clear that many stars have velocities not consistent with pure circular orbits as prescribed by differential rotation. The latitude distribution, together with the $l - v$ distribution indicates that the group I sources have a larger scale-height in the z direction and larger velocity dispersions than the group II sources. In section 5 we will show indeed that the two groups have quite different distribution functions.

$$\begin{aligned}\mu_{ob}(\mathbf{x}_l, \mathbf{v}_l) &= \int_{\tau l} \mu(\mathbf{x}, \mathbf{v}) F(\mathbf{I}) d\mathbf{x} d\mathbf{v} \\ &= \sum_i c_i \int_{\tau l} \mu(\mathbf{x}, \mathbf{v}) F_i(\mathbf{I}) d\mathbf{x} d\mathbf{v} \\ &= \sum_i c_i \mu_i(\mathbf{x}_l, \mathbf{v}_l)\end{aligned}$$

Then we can define the quantity χ^2:

$$\chi^2 = \sum_l w_l \left(\mu_{ob}(\mathbf{x}_l, \mathbf{v}_l) - \sum_i c_i \mu_i(\mathbf{x}_l, \mathbf{v}_l) \right)^2 .$$

The program minimizes χ^2 by fiddling around with the coefficients c_i with the additional constraint that the distribution function be positive. The coefficients c_i are determined with a quadratic programming algorithm as described in paper I.

In preparation for the modelling we define boxes (identical to the volume elements 'τ_l' in the previous section) in Galactic co-ordinates, each containing about 20 stars, which are chosen, for *IRAS*, in unconfused areas in the sky. We subdivide the sample into rectangular bins in the plane of the sky, each bin containing approximately 20 stars. For each bin, we calculate the (projected) density, mean velocity and velocity scatter (zeroth, first and second moment of the velocity distribution) along the line-of-sight. This yields three observables for each bin: the $\mu_{ob}(\mathbf{x}_l, \mathbf{v}_l)$ in the previous section. Errors are calculated using the normal estimates assuming a gaussian distribution. Since we assume that the distribution of the stars is axisymmetric, we used the differences in the observables between the four quadrants for a further uncertainty estimate; these uncertainties are used in the weight coefficients (w_l) of the statistical χ^2 variable (see previous section).

5. Results

The best fits to the two samples of OH/IR stars have χ^2 well within the 10% confidence limit and are thus compatible with the data. In Figure 6 we show in grey-scale representation the distribution of orbits in the E_b, L_z plane. For $E_b \lesssim 0.6$ there is a strong concentration to the left boundary for the bound orbits, indicating that all orbits are approaching circular orbits with radii $\gtrsim$ 2.5 kpc. However, as we have noticed before, even when L_z deviates by a relatively small amount from its maximum value (that of a circular orbit) the star begins to make large excursions in the longitude–velocity diagram (Figures 1, 2 and 3). For $E_b \gtrsim 0.6$ the orbits begin to fill all available E_b, L_z space. This means that for $\varpi \lesssim 2.5$ kpc (compare Figures 6 and 1) radial and counter-rotating orbits begin to occur, although there is still a majority of orbits in the 'normal' sense of rotation (i.e., co-rotating). The differences between group I sources and group II sources in Figure 6 show that the orbits of group I sources deviate significantly more from circularity than those of group II, confirming the conclusion that they are of lower ZAMS-mass. The distribution functions do not show counter-rotating orbits, except for points in phase space with small L_z and high binding energy E_b(for $\varpi < 2.5$ kpc, which describes the orbits of stars in the bulge of the galaxy).

The distribution functions represented in Figure 6 allow us to calculate by integration the moments of F, yielding such quantities as the (local) stellar density, average velocity and velocity dispersions. In Figure 7 we give the mean angular velocity, and in Figure 8 the velocity dispersions (σ_φ and σ_ϖ) as function of galactocentric distance ϖ in the plane $z = 0$. The confidence limits on the plotted curves can be estimated by comparing the best fit models with models near the 1% confidence limit (this is equivalent to 3σ, assuming a gaussian distribution). Within 1 kpc from the centre the uncertainties in the dispersions are 30 km s^{-1}; from 1–3 kpc, 15 km s^{-1}; beyond 2 kpc, about 10 km s^{-1}. For the velocities the error bars are 25, 10 and 5 km s^{-1} respectively.

Figures 7 and 8 confirm what we concluded above from Figure 6: (1) that the two groups, I and II, differ in their kinematical properties, and (2) that inside 2.5 kpc ($E_b \gtrsim 0.6$) orbits of different character (radial and counter-rotating) begin to occur. At radii larger than $\approx$ 4 kpc the two groups behave similarly: there is a (nearly) constant difference in velocity and in the

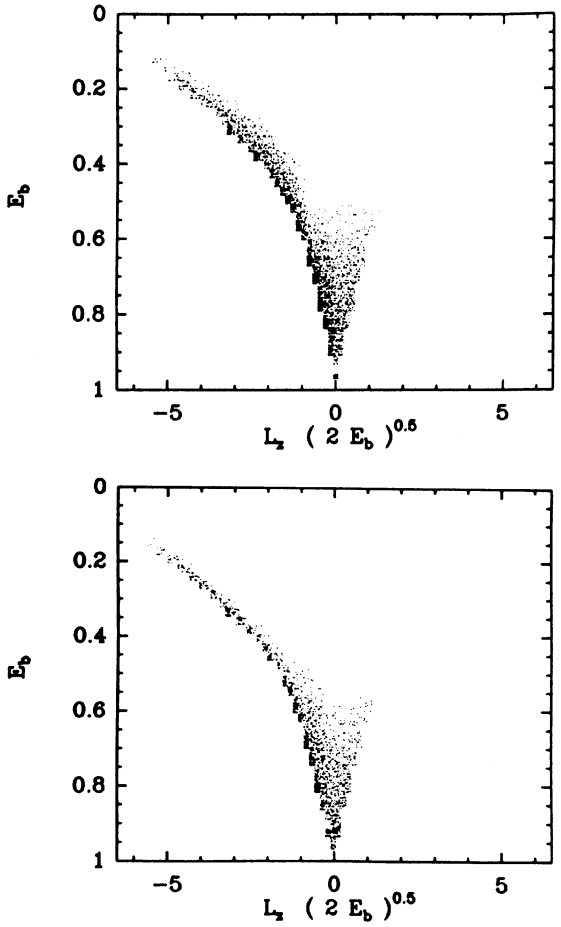

Figure 6: *Top* – The distribution function for the group I OH/IR stars. The degree of shading is proportional to the logarithm of the distribution function value. *Bottom* – The distribution function for the group II OH/IR stars.

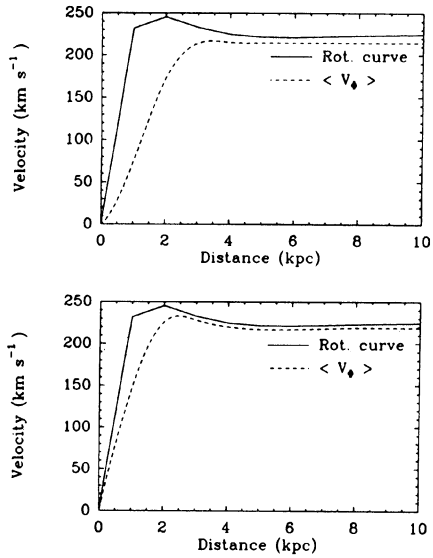

Figure 7: *Top* – The mean angular velocity ($\langle v_\varphi \rangle = \mu_\varphi$) as function of galactocentric distance (ϖ) in the plane $z = 0$, for the OH/IR stars of group I. *Bottom* – As above, for the group II OH/IR stars.

dispersions. At 8 kpc from the centre, $\sigma_\varpi \approx 49\,\mathrm{km\,s^{-1}}$ and $\sigma_\varphi \approx 41\,\mathrm{km\,s^{-1}}$ for group I are both larger than for group II for which $\sigma_\varpi \approx 29\,\mathrm{km\,s^{-1}}$ and $\sigma_\varphi \approx 27\,\mathrm{km\,s^{-1}}$. The asymmetric drift at 8 kpc from the centre is similar for both groups: $10\,\mathrm{km\,s^{-1}}$.

Within 4 kpc from the centre the velocity dispersions in ϖ and φ are quite different for the two groups. The velocity dispersions of group II only rise within 1 to 2 kpc from the centre. Consequently the mean angular velocity drops. The velocity dispersions of group I rises sharply for $\varpi \lesssim 3$ kpc.

We derive the z scale-heights at 8 kpc from the centre (defined as the height where the volume mass density drops to 50% of the value in the disc) for both groups and we find 1200 pc for group I and 500 pc for group II. These values are consistent with the Galactic density models for an *IRAS* sample of AGB stars of Habing (1988).

6. Discussion and Conclusions

The velocity dispersions in the solar neighbourhood can be used to estimate the average age for each group using Wielen's (1977) empirical relation between velocity dispersions and ages, based on stellar groups in the solar neighbourhood (see his Figure 1). We find 10 Gyr for group I and 5 Gyr for group II. Information on the masses can then be derived from stellar evolution models as discussed, for example, in the review by Iben and Renzini (1983). The ensuing ZAMS masses from these ages are 1–2 $M_\odot$. Corroborating evidence for such masses is found in Habing (1987), who finds luminosities for AGB stars in the bulge of around 5000 $L_\odot$. This is consistent with a ZAMS mass of about 1 $M_\odot$ (Iben and Renzini 1983) and it suggests that they are old enough to be dynamically relaxed.

The velocity dispersions and z scale-heights derived for group I are fairly similar to those found for the so-called thick disc (e.g., Gilmore, Wyse and Kuijken 1989, and references therein), except for the asymmetric drift (estimated to be about $45\,\mathrm{km\,s^{-1}}$ for the thick disc). In this regard there is better agreement with the the kinematics of the thick disc as derived by Ratnatunga and Freeman (1989) from a sample of K-giants: $25\,\mathrm{km\,s^{-1}}$. The group II fit well within the observed kinematical properties for the so-called old disc (see Freeman 1987, and references therein). Thus, the *IRAS* sample of OH/IR stars represents an old, low mass population (see also Likkel 1989).

It is unlikely that the group I and II stars originate from the same population, i.e., arise from a similar initial Galactic distribution. Collisional heating effects in the Galactic disc, e.g., by molecular clouds, are probably unable to bridge the fairly large difference in the calculated velocity dispersions (Lacey 1984; Villumsen 1985). Patchy spiral arms (Carlberg and Sellwood 1985) may be somewhat more effective (see also in this context the discussion in te Lintel Hekkert and Dejonghe 1989). None of these mechanisms can explain both the increase of the velocity dispersions and the increase of the z scale-height.

The data, as interpreted here, show clearly different population characteristics from those used by Baud (1981a; 1981b) for his sample of OH/IR stars obtained by means of 'blind' surveys. For both groups (I and II) the velocity dispersions are higher and the z scale-height is larger than for his sample. The difference appears to be real and is connected with the way the samples were selected.

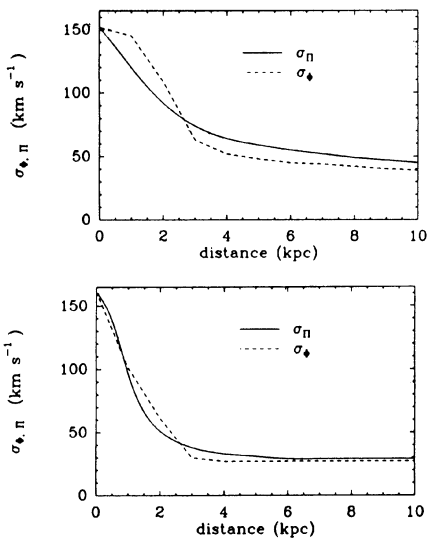

Figure 8: *Top* – For the group I OH/IR stars σ_φ and σ_r as function of ϖ in the plane $z = 0$. *Bottom* – As above, for the group II OH/IR stars.

Acknowledgement

PLH acknowledges the hospitality of the Institute of Advanced Studies, Princeton. It is a pleasure to thank H. Steyaert for his hospitality during the many visits of PLH to Gent. We are grateful to the computing staff of the CDR, Gent, for their constant assistance. We are pleased to thank Professor J. H. Oort for his comments and interest in the project. Phil Maloney is gratefully acknowledged for critically reading many versions of the manuscript. The Leidse Kerkhoven Bosscha Fonds (LKBF) and Netherlands Foundation for Research (NWO) financed in part the travel of PLH to Princeton and Gent.

Baud, B., Habing, H. J., Matthews, H. E., Winnberg, A., 1981, *Astron. Astrophys.*, **95**, 156.
Baud, B., Habing, H. J., Matthews, H. E., Winnberg, A., 1981b, *Astron. Astrophys.*, **95**, 171.
Bahcall, J. N., Schmidt, M., Soneira, R. M., 1982, *Astrophys. J. Lett.*, **258**, L23.
Binney, J., Tremaine, S., 1987, *Galactic Dynamics*, Princeton University Press, Princeton.
Burton, W. B., Gordon, M. A., 1978, *Astron. Astrophys.*, **63**, 7.
Carlberg, R. G., Sellwood, J. A., 1985, *Astrophys. J.*, **292**, 79.
Dejonghe, H., 1989, *Astrophys. J.*, **343**, 113. (Paper I)
Dejonghe, H., de Zeeuw, P. T.1988, in *Mass of the Galaxy*, ed. M. Fich, (Toronto University Press), p 55.
Eder, J., Lewis, B. M., Terzian, Y., 1988, *Astrophys. J. Suppl.*, **66**, 183.
Feast, M. 1987, in *Galaxy*, eds. G. Gilmore and B. Carswell (Reidel, Dordrecht), p 1.
Freeman, K., 1987, *Annu. Rev. Astron. Astrophys.*, **25**, 603.
Fricke, W., 1952, *Astron. Nachr.*, **280**, 193.
Gilmore, G., Wyse, R. F. G., Kuyken, K., 1989, *Annu. Rev. Astron. Astrophys.*, **27**, 555.
Habing, H. J., 1987 1987, in *Late stages of stellar evolution*, eds. S. Kwok and S. R. Pottasch, (Reidel, Dordrecht), p 291.
Habing, H. J., 1988, *Astron. Astrophys.*, **200**, 40.
Herman, J., 1988, *Astron. Astrophys. Suppl. Ser.*, **74**, 133.
Iben Jr., I., Renzini, A., 1983, *Annu. Rev. Astron. Astrophys.*, **21**, 271.
Lacey, C. G., 1984, *Mon. Not. R. Astr. Soc.*, **208**, 687.
Likkel, L., 1989, *Astrophys. J.*, **344**, 350.
te Lintel Hekkert, P., Habing, H. J., Caswell, J. L., Norris, R. P., Haynes, R. F., 1989a, *Astron. Astrophys. Suppl. Ser.*, submitted.
te Lintel Hekkert, P., Sivagnanam, P., Habing, H. J., Le Squeren, A. M., 1989b, in preparation.
te Lintel Hekkert, P., Dejonghe, H.1989, in *Astrophysical Discs*, ed. J. R. Sellwood, (Reidel, Dordrecht), in press.
Olnon, F. M., 1977, PhD thesis, Leiden University.
Olnon, F. M., Walterbos, R. A. M., Habing, H. J., Matthews, H. R., Winnberg, A., Brzezinska, H., Baud, B., 1981, *Astrophys. J. Lett.*, **245**, L103.
Sivagnanam, P., Le Squeren, A. M., 1986, *Astron. Astrophys.*, **168**, 374.
Ratnatunga, K. U., Freeman, K. C., 1989, *Astrophys. J.*, **339**, 126.
van der Veen, W. E. C. J., Breukers, R., 1989, *Astron. Astrophys.*, **213**, 133.
Villumsen, J. V., 1985, *Astrophys. J.*, **290**, 75.
Wielen, R., 1977, *Astron. Astrophys.*, **60**, 263.